Supplemental Document for Paper “ComplexGen: CAD Reconstruction by B-Rep Chain Complex Generation”

HAOXIANG GUO, Tsinghua University, and Microsoft Research Asia, China
SHILIN LIU, University of Science and Technology of China, and Microsoft Research Asia, China
HAO PAN, YANG LIU, XIN TONG, and BAINING GUO, Microsoft Research Asia, China

1 PROOF OF SUFFICIENCY OF INTEGER PROGRAM CONSTRAINTS

We prove that the constraints of the chain complex extraction problem in the main text are sufficient for describing all the dependencies between unary variables that model per-element validness and topology variables that model the adjacency of pairs of elements.

First, we reproduce the topological constraints from the main text here, for ease of reference.

$$\sum_i \mathbf{FE}[i,j] = 2\mathbf{E}[j], \tag{1}$$

$$\sum_j \mathbf{EV}[i,j] = 2\mathbf{E}[i]\mathbf{O}[i], \tag{2}$$

$$\mathbf{FE} \times \mathbf{EV} = 2\mathbf{FV} \tag{3}$$

$$\mathbf{FE}[i,j] \le \mathbf{F}[i], \tag{4}$$

$$\mathbf{EV}[i,j] \le \mathbf{V}[j] \le \sum_k \mathbf{EV}[k,j], \tag{5}$$

Next, we list the complete set of constraints that describe all dependencies between unary variables and binary variables explicitly and may contain redundancies:

$$\mathbf{FE}[i,j] \le \mathbf{F}[i] \tag{6}$$

$$\mathbf{FE}[i,j] \le \mathbf{E}[j] \le \sum_k \mathbf{FE}[k,j] \tag{7}$$

$$\mathbf{EV}[i,j] \le \mathbf{E}[i] \tag{8}$$

$$\mathbf{EV}[i,j] \le \mathbf{V}[j] \le \sum_k \mathbf{EV}[k,j]$$

$$\mathbf{FV}[i,j] \le \mathbf{F}[i] \tag{9}$$

$$\mathbf{FV}[i,j] \le \mathbf{V}[j] \le \sum_k \mathbf{FV}[k,j] \tag{10}$$

Note that here we allow for faces that are closed and therefore have no adjacent edges or vertices, hence the missing right parts for face inequalities (4),(6),(9). However, the case of requiring faces to always have adjacent edges and vertices can be analyzed in a similar way as what follows.

We show that the constraints in (6-10) and absent from (1-5) are indeed redundant, in the sense of being derivable from the constraints of (1-5). We analyse the inequalities one-by-one.

Authors' addresses: H. Guo, Tsinghua University, Haidian District, Beijing, China; ghx17@mails.tsinghua.edu.cn; S. Liu, University of Science and Technology of China, Hefei, China; freelin@mail.ustc.edu.cn; H. Pan (corresponding author), Y. Liu, X. Tong, B. Guo, 5 Danling St., Haidian District, Beijing, China; {haopan, yangliu, xtong, baining}@microsoft.com.

Table 1. Detection accuracy with geometry embedding modules implemented by conditioned MLP or hypernet. The results are comparable in most aspects except for patch F-score where hypernet obtains a 1.4% improvement.

Config	Corner↑	Curve↑			Patch↑			Topology error↓			Topo inconsistency↓		
	F-score	F-score	Type acc	Open acc	F-score	Type acc	Open acc	FE	FV	EV	|(1)|	|(2)|	|(3)|
MLP	80.2	**75.3**	**77.2**	**95.3**	77.4	**76.9**	**94.2**	**0.126**	**0.111**	**0.16**	0.962	0.618	0.167
Hypernet	**80.9**	75.2	76.9	94.8	**78.8**	76.2	93.6	0.145	0.131	0.174	**0.873**	**0.608**	**0.154**

Redundancy of (7). From (1) it is clear that for binary variables $\mathbf{E}, \mathbf{FE}$ the inequality (7) holds. For when $\mathbf{E}[j] = 0$, by (1) it is necessary that $\mathbf{FE}[i, j] = 0, \forall i$, hence we have (7); otherwise when $\mathbf{E}[j] = 1$, $\sum_k \mathbf{FE}[k, j] = 2$ by (1) and thus (7) still holds.

Redundancy of (8). From (2), we have $\sum_j \mathbf{EV}[i, j] = 2\mathbf{E}[i]\mathbf{O}[i] \leq 2\mathbf{E}[i]$. An examination of the binary cases of $\mathbf{E}[i]$ shows that (8) holds as a result.

Redundancy of (9). Again we enumerate the binary cases of $\mathbf{F}[i]$. When $\mathbf{F}[i] = 0$, by (4) we have that $\mathbf{FE}[i, j] = 0$; as a result, by (3) we have $\mathbf{FV}[i, k] = 0, \forall k$, hence (9). When $\mathbf{F}[i] = 1$, (9) trivially holds for binary variables.

Redundancy of (10). When $\mathbf{V}[j] = 0$, by (5) we have $\mathbf{EV}[i, j] = 0, \forall i$. Further by (3), we have $2\mathbf{FV}[k, j] = \sum_i \mathbf{FE}[k, i] \cdot \mathbf{EV}[i, j] = 0, \forall k$.

When $\mathbf{V}[j] = 1$, by (5) there exists i such that $\mathbf{EV}[i, j] = 1$. From (1) we have that there exists m, l such that $\mathbf{FE}[m, i] + \mathbf{FE}[l, i] = 2\mathbf{E}[i] = 2$. For the faces m, l, we thus have that $2\mathbf{FV}[m, j] \geq \mathbf{FE}[m, i] \cdot \mathbf{EV}[i, j] = 1$ as well as $2\mathbf{FV}[l, j] \geq \mathbf{FE}[l, i] \cdot \mathbf{EV}[i, j] = 1$, where $\mathbf{FV}$ is expanded according to (3). As a result, $\sum_k \mathbf{FV}[k, j] \geq \mathbf{FV}[m, j] + \mathbf{FV}[l, j] = 2 \geq \mathbf{V}[j]$.

The two parts conclude the proof of (10).

2 HYPER NETWORK FOR GEOMETRY EMBEDDING

We adopt hyper networks [Ha et al. 2017] for implementing the unified mappings of curve and patch geometry embeddings (Sec. 4.1 of main text). An alternative choice is to use conditioned MLPs, where the latent code of an element is concatenated with the parameter code and mapped to 3D coordinates by an MLP, akin to the Atlasnet formulation [Deprelle et al. 2019].

With comparable amounts of trainable parameters, our choice of hypernet over conditioned MLP is based on two observations: 1) hypernet achieves slightly better accuracy than conditioned MLP, and 2) hypernet consumes fewer intermediate storage than conditioned MLP. The better accuracy of hypernet is shown in Table 1, where we see an improvement of 1.4% for patch F-score. Meanwhile, given comparable amounts of parameters, conditioned MLP has many more intermediate layers (*e.g.*, 5 intermediate layers with feature size 192) than hypernet which is a 3rd-order tensor product structure in each layer; this is further scaled by the large numbers of patch sample points (100 per patch), which together leads to significantly more memory consumption by MLP for backward propagation during training.

3 MORE RESULTS

We show more results of different complexities in Fig. 1.

4 DATA CLEANING

CAD models in ABC dataset have several common problems that need to be fixed for generating proper and unambiguous training pairs of input point cloud and output B-Rep structure. The problems include:

(1) Open boundary models.
(2) Lines, circles denoted as splines.

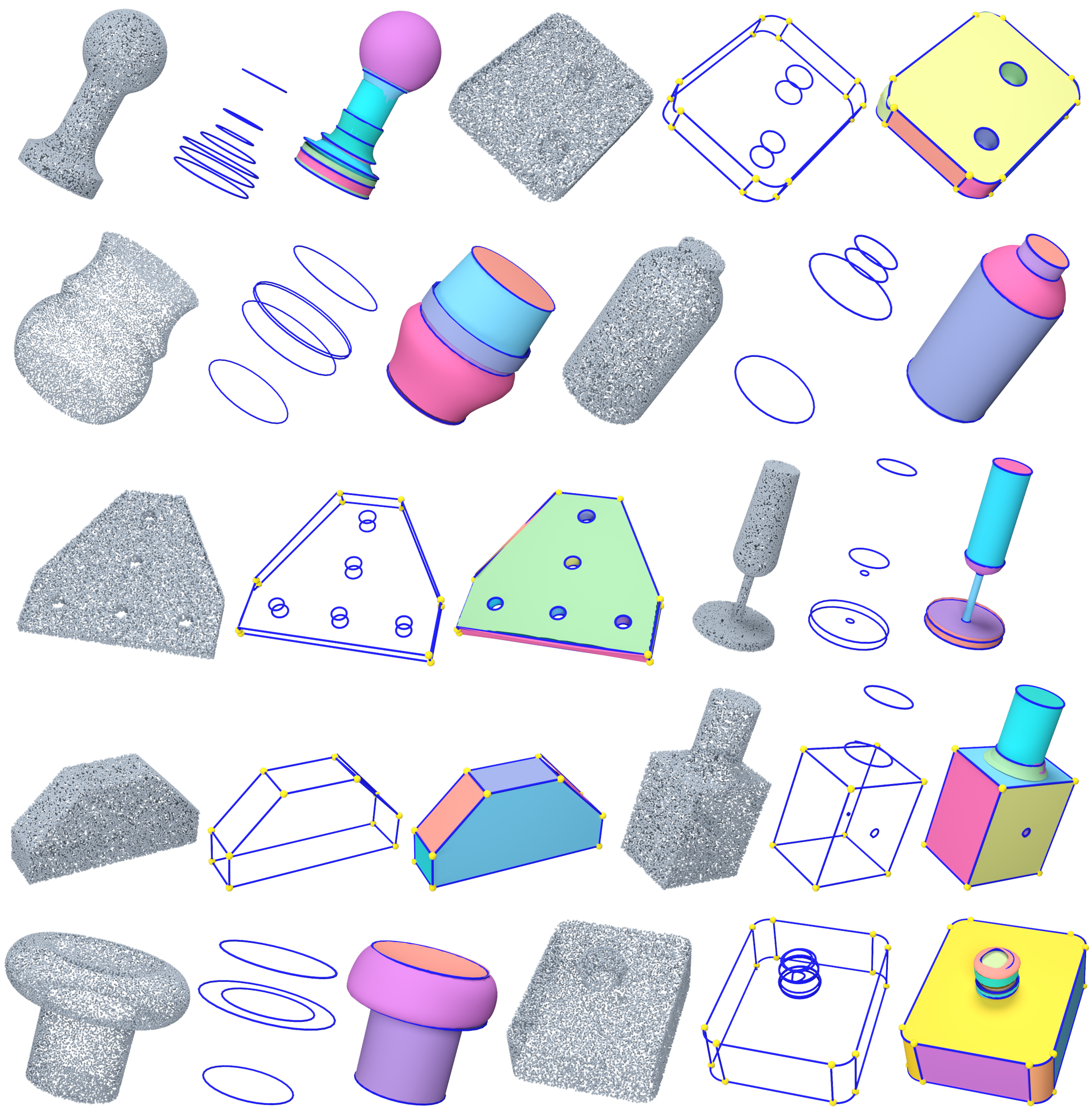

Fig. 1. More results of diverse complexities from the test set.

(3) Over-segmentation of patches (curves) by junctions whose neighboring patches (curves) have identical types and geometry, which represents ambiguous structures undetectable from the input geometry. For example, consider a cylinder split by arbitrary profile lines.
(4) Unknown patch types.

(5) Parametric representations of patches do not match their discrete mesh representation, which causes problem for ground-truth patch grid generation (Sec. 4.2 of main text).
(6) Disconnected components in one model. The components frequently overlap spatially, leading to self-intersecting and ambiguous models.

To address these issues, we remove the open boundary models, models with unknown patch types or with mismatched parametric and mesh representations, apply line and circle fitting to curves to determine if they are lines/circles rather than the more general splines, and merge the over-segmented patches/curves. Finally, we split a model with disconnected components into multiple models, each containing a single component.

REFERENCES

Theo Deprelle, Thibault Groueix, Matthew Fisher, Vladimir Kim, Bryan Russell, and Mathieu Aubry. 2019. Learning elementary structures for 3D shape generation and matching. In *Advances in Neural Information Processing Systems*.

David Ha, Andrew Dai, and Quoc V. Le. 2017. HyperNetworks. In *ICLR*.